

NONLINEAR ANALYSIS OF REINFORCED CONCRETE BEAM GRIDS



Mikko Kilpeläinen
University of Oulu, Finland,
Department of Civil Engineering
Caretaker professor of building
construction technology

A method for nonlinear structural analysis of reinforced concrete beam grids is presented in this paper. First, the factors, such as σ - ϵ curves, cracking of concrete and yielding of reinforcement causing the nonlinear behaviour of that kind of structures are examined. Flexural and torsional stiffnesses are defined as a secant stiffness from tri-segmentally approximated moment-curvature and torque-twist curves, respectively. The method itself is based on the finite beam element method and load increment technique with iteration. Computational results are compared with some test results. Observations and suggestions on the basis of the comparison are reported.

Keywords: cracking, flexural stiffness, torsional stiffness, element method

1. INTRODUCTION

For the nonlinear analysis of reinforced concrete structures, many different procedures have been developed. Most of them are based on the finite element method and load increment technique. The nonlinear analysis of various structures, however, has many various problems. Therefore, different methods and computer programs are required for the solution of nonlinear problems of different structures, such as beams, plates, frames, shells etc. Although beam grids are broadly composed of a slab and beams, the methods for the analysis of plate and beam structures cannot be used directly in the analysis of beam grids. Since methods specifically intended for the nonlinear analysis of reinforced concrete beam grids was non-existent, an investigation was regarded as requisite to filling this gap. It was performed at the University of Oulu /1/ and its purpose was to develop a method applicable to the nonlinear structural analysis of reinforced concrete beam grids. This paper is based on the results of that investigation. Its purpose is to describe the method of analysis and to present some findings received through the calculations.

2. ASSUMPTIONS AND LIMITATIONS

In order to simplify the method of analysis many assumptions and limitations have been made. The most important principles, assumptions and limitations linked with this method are the following:

1. The method is based on the finite element method. The elements are unidimensional beam elements. Two- and three-dimensional states of stress are not examined.
2. The geometry of the beam grid may be arbitrary (skew, rectangular, different lengths of elements, simply supported or continuous beam etc.). However, the cross-section of the elements will be rectangular or L- or T-shaped and uniform along the entire element.
3. The load is assumed to be situated in the nodal points of the elements as point loads affecting the beam grid plane perpendicularly.
4. Loading will be of short duration, increasing monotonously.
5. The beams are assumed to be underreinforced. The reinforcement of the beams shall be known prior to analysis. The quantity and location of the reinforcement will not be altered during calculation. The stirrups must be vertical when used. Otherwise the reinforcement may be arbitrary.
6. The supports may be clamped or hinged in the direction of each degree of freedom.
7. The member ends may be released. Plastic hinges may arise during the calculation at the ends of elements due to the yielding of reinforcement. A hinge may be flexural, torsional or shear hinge, or a combination of these.
8. The torque in the elements is assumed to be free in character, ie. the cross-section will be warped due to the torque.
9. The plane sections of the beam elements will remain as planes in bending.
10. The shear rigidity of the beams will not be taken into account in the formation of the stiffness matrix of the beam element.
11. The creep of concrete will not be taken into the consideration.

3. STRESS-STRAIN CHARACTERISTICS OF CONCRETE AND STEEL

3.1. Compressed concrete

The nonlinear stress-strain curve of compressed concrete is approximated through the polynom

$$\sigma_c = a_0 + a_1 \cdot \eta + a_2 \cdot \eta^2 + a_3 \cdot \eta^3 + a_4 \cdot \eta^4 \quad (1)$$

The coefficients $a_0 \dots a_4$ are determined according to the

following boundary conditions:

1. $\sigma_c = 0$, when $\epsilon_c = 0$
2. $\sigma_c = f'_c$, when $\epsilon_c = \epsilon_{cy}$
3. $\sigma_c = 0,85 \cdot f'_c$, when $\epsilon_c = \epsilon_{cu}$ (2)
4. $\frac{d\sigma_c}{d\epsilon_c} = E_c$, when $\epsilon_c = 0$
5. $\frac{d\sigma_c}{d\epsilon_c} = 0$, when $\epsilon_c = \epsilon_{cy}$

By employing the equations

$$\eta = \frac{\epsilon_c}{\epsilon_{cy}}$$

$$E_c = 6200 \cdot \sqrt{f'_c} \quad (3)$$

$$\epsilon_{cy} = 2,0 \%$$

$$\epsilon_{cu} = 3,9 - 0,02 \cdot f'_c \%$$

we derive the stress-strain curves as shown in Fig. 1a for the various strengths of concrete. The stress-strain curves in Fig. 1a are used in this study for the calculation of the cracking and yielding moments of the beam element in pure flexure.

3.2. Tensioned concrete

The stress-strain curve of tensioned concrete is approximated through the polynomial

$$\sigma_{ct} = b_0 + b_1 \cdot \eta + b_2 \cdot \eta^2 + b_3 \cdot \eta^3 \quad (4)$$

The boundary conditions for the determination of coefficients $b_0 \dots b_3$ are the following:

1. $\sigma_{ct} = 0$, when $\epsilon_{ct} = 0$
2. $\sigma_{ct} = f_{ct}$, when $\epsilon_{ct} = \epsilon_{cty}$
3. $\frac{d\sigma_{ct}}{d\epsilon_{ct}} = E_c$, when $\epsilon_{ct} = 0$ (5)

$$4. \quad \frac{d\sigma_{ct}}{d\epsilon_{ct}} = 0, \quad \text{when} \quad \epsilon_{ct} = \epsilon_{cty}$$

When we employ the equations

$$\eta = \frac{\epsilon_{ct}}{\epsilon_{cty}}$$

$$E_c = 6200 \cdot \sqrt{f'_c}$$

(6)

$$\epsilon_{cty} = \epsilon_{ctu} = 0,175 \%$$

$$f_{ct} = 0,30 \cdot \sqrt[3]{f'_c{}^2},$$

we acquire the curves of Fig. 1b between the flexural tensile stress and strain of concrete. In the cases involving concentric tension, tensile strength is calculated from the equation

$$f_{ct} = 0,25 \cdot \sqrt[3]{f'_c{}^2}$$

(7)

The curves shown in Fig. 1b are utilized for the calculation of the cracking moment of the beam element in both pure flexure and in pure torsion. In determining the cracking shear force in pure shear, Eq. (7) is used.

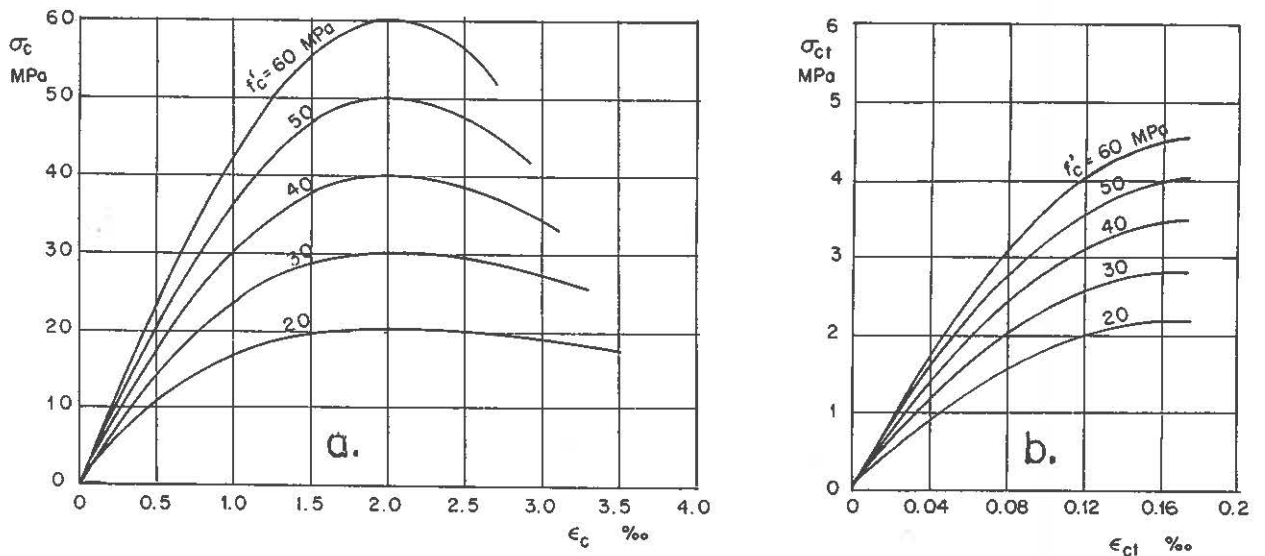


Fig. 1. The σ - ϵ curves of compressed (a) and flexurally tensioned (b) concrete.

3.3. Steel

The stress-strain curve of steel is assumed to be in accordance

with Fig. 2. In other words, the steel is assumed to be elasto-plastic material. The strain-hardening is not taken into the consideration.

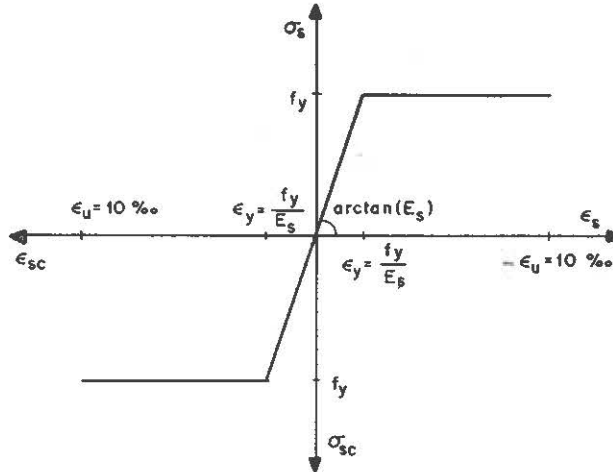


Fig. 2. The σ - ϵ curves of reinforcement in tension and compression.

4. CRACKING CAPACITY OF REINFORCED CONCRETE BEAM SECTION

4.1. Pure bending

The positive flexural cracking moment of a reinforced concrete beam section in pure bending is obtained from the equation

$$M_{\text{ropos}} = \int_{A_{cc}} \sigma_c(\epsilon_c) \cdot \frac{\epsilon_c}{\epsilon_{cc}} \cdot x \cdot dA + \int_{A_{ct}} \sigma_{ct}(\epsilon_{ct}) \cdot \frac{\epsilon_{ct}}{\epsilon_{cty}} \cdot (h-x) \cdot dA + D_s \cdot (x-d') + Z_s \cdot (d-x) \quad (8)$$

The internal stress resultants can be calculated first in normal way using equilibrium equation within iteration. The notation is clarified in Fig. 3.

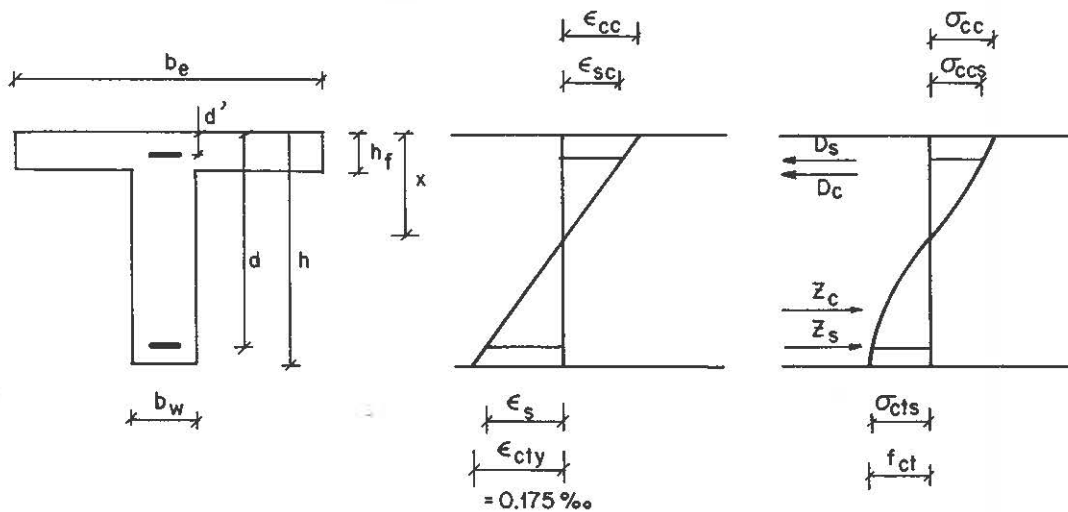


Fig. 3. Stress and strain diagrams of the beam section as the cracking of concrete commences in pure flexure. $M > 0$.

The negative flexural cracking moment is obtained in the same way. The compression is now at the lower edge of the section.

In accordance with Eq. (8), the flexural cracking moment for 28 test beams were calculated, of which the test results can be found in the literature. The calculated values were compared with the experimentally obtained values. The mean and the standard deviation of the ratios M_{rotest} / M_{rocalc} were 0,970 and 0,435, respectively.

4.2. Pure torsion

The torsional cracking moment is normally calculated approximately by application of either the theory of elasticity or the theory of plasticity. In this investigation, the nonlinear method is used. The derivation of the method has been presented in Ref. /1/. The cracking of concrete begins generally at the longer edge of the web. At this time, the rigidity of the web is assumed to be 60 % of its linearly elastic value, as shown by many test results. So we have the equation

$$K_{trw} = 0,60 \cdot G_c \cdot \left(\frac{1}{3} - \frac{0,23}{0,18 + \frac{h}{b_w}} \right) \cdot h \cdot b_w^3 \quad (9)$$

At same time, the rigidity of the flanges is assumed to be 80 % of their linearly elastic values. The torsional rigidities of the flanges are obtained thereby from the equation

$$K_{trf} = 0,267 \cdot G_c \cdot h_f^3 \cdot b_f \quad (10)$$

The total rigidity of the section, when the cracking commences, is derived from the equation

$$K_{tro} = k \cdot (K_{trw} + \sum_1^2 K_{trf}) \quad , \quad (11)$$

when for the T-section $k = 1,15$ and for the L and rectangular sections $k = 1,0$.

The torsional cracking moment in pure torsion for the whole section is obtained from the equation

$$T_{ro} = \frac{K_{tro}}{K_{trw}} \cdot f_{ct} \cdot W_{tpw} \quad (12)$$

The nonlinear torsional resistance of the web W_{tpw} is derived to be $1,33 \cdot W_t$, when W_t is calculated according to W_{tpw} the theory of elasticity. Thus we have the equation

$$T_{ro} = 1,33 \cdot \frac{K_{tro}}{K_{trw}} \cdot f_{ct} \cdot \frac{h \cdot b_w^2}{3,0 + \frac{2,6}{0,45 + \frac{h}{b_w}}} \quad (13)$$

In the middle of the shorter side of the web, the cracking is presumed to start when the torsional moment secures the value

$$T'_{ro} = 1,33 \cdot \frac{K_{tro}}{K_{trw}} \cdot f_{ct} \cdot \frac{0,54}{1,60 + \frac{h}{b_w}} \cdot h^2 \cdot b_w \quad (14)$$

T'_{ro} is the computational torsional cracking moment when examining the combined influence of torsion and bending.

By utilizing Eq. (13) the torsional cracking moment for 78 test beams were calculated, the test results of which could be found in the literature. The values calculated were compared to the values experimentally obtained. The mean and the standard deviation of the ratios $T_{ro\text{test}}/T_{ro\text{calc}}$ were 0,981 and 0,178 for all beams, 1,011 and 0,127 for T-beams, 1,025 and 0,193 for L-beams and 0,922 and 0,206 for rectangular beams, respectively.

4.3. Pure shear

The cracking shear force in pure shear is obtained from the equation

$$V_{ro} = f_{ct} \cdot b_w \cdot z \quad (15)$$

f_{ct} is obtained from Eq. (7) and z from the equation

$$z \approx z_{ro} = \frac{|M_{ro}|}{Z_s + Z_c} = \frac{|M_{ro}|}{D_s + D_c} \quad (16)$$

The comparison of the calculational results with the experimental results of 31 test beams found in the literature showed poor correspondence. Since cracking shear force is dependent on the shear span a as well as on the effective depth d of the beam, the better calculational result for V_{ro} can be obtained from the equation

$$V_{ro} = (1,0 - \frac{(\frac{a}{d})^{4,8}}{29} \cdot e^{-\frac{a}{d}}) \cdot f_{ct} \cdot b_w \cdot z_{ro} \quad (17)$$

Eq. (17) has been derived using heuristic curve fitting within test results of 31 test beams. Employing Eq. (17), the mean and standard deviation of $V_{ro\text{test}}/V_{ro\text{calc}}$ -ratios of those test beams were 0,988 and 0,193, respectively.

4.4. Combined flexure and torsion

Cracking appears in concrete due to the combined influence of the flexural moment and the torsional moment on the flexurally tensioned edge of the section. The flexural stress σ and shear stress τ realize, as cracking begins, the equation

$$\sigma_1 = f_{ct} = \frac{\sigma}{2} + \frac{1}{2} \cdot \sqrt{\sigma^2 + 4 \cdot \tau^2} \quad (18)$$

when cracking is assumed to appear, as the principal tensile stress surpasses the tensile strength of the concrete. When σ and τ are approximately obtained from the equations

$$\sigma = \frac{M_r}{M_{ro}} \cdot f_{ct} \quad (19)$$

$$\tau = \frac{T_r}{T_{ro}} \cdot f_{ct}$$

we obtain, using Eqs. (18) and (19), the equation

$$\frac{M_r}{M_{ro}} + \left(\frac{T_r}{T_{ro}}\right)^2 = 1 \quad (20)$$

Eq. (20) indicates the interaction of the flexural moment M_r and the torsional moment T_r , as cracking appears.

The interaction between the flexural and torsional moments,

calculated in accordance with Eq. (20), were compared with the test results of 62 test beams found in the literature. For each test beam, the left side value of Eq. (20) was calculated in the form $M_{rtest}/M_{rocalc} + (T_{rtest}/T'_{rocalc})^2$. The mean and the standard deviation of those values were 1,065 and 0,537, respectively.

4.5. Combined torsion and shear

If we assume that the shear stresses caused by torsion and shear obtain their maximum value at the same point, and, if we use principal tensile stress criterion for cracking, then the equation

$$\sigma_1 = f_{ct} = \tau_t + \tau_v \quad (21)$$

is valid.

We can approximately write the expressions

$$\tau_t = \frac{T_r}{T_{ro}} \cdot f_{ct} \quad (22)$$

$$\tau_v = \frac{V_r}{V_{ro}} \cdot f_{ct}$$

Thus we have the equation

$$\frac{T_r}{T_{ro}} + \frac{V_r}{V_{ro}} = 1 \quad (23)$$

which shows the interaction of the torsion and the shear, as cracking in the concrete begins.

The comparison of the calculational results with the test results of 69 test beams found in the literature showed, however, that the equation

$$\left(\frac{T_r}{T_{ro}}\right)^2 + 0,40 \cdot \frac{T_r}{T_{ro}} \cdot \frac{V_r}{V_{ro}} + \left(\frac{V_r}{V_{ro}}\right)^2 = 1 \quad (24)$$

gives better correspondence between calculational and experimental results. The left side value of Eq. (24) was calculated for each test beam using ratios T_{rtest}/T_{rocalc} and V_{rtest}/V_{rocalc} . The mean and the standard deviation of those values were 1,002 and 0,372, respectively.

5. ULTIMATE CAPACITY OF A REINFORCED CONCRETE BEAM SECTION

In addition to the nonlinear stress-strain curve of concrete and to the cracking of concrete, the yielding of reinforcement causes nonlinearity in the behaviour of reinforced concrete structures. The ultimate capacity of a reinforced concrete beam section is defined as the loading which causes the yielding of the reinforcement. A well-established basis for the capacity calculations in combined loading is truss analogy. The beams are examined as a space truss, of which the longitudinal reinforcement located in the corners of the section and the vertical stirrups function as tensioned rods, and the concrete between the skew cracks act as diagonal compressed struts. The ultimate capacity of flanged beams or of beams having small T/M-ratio, as generally in beam grids, calculated in accordance with the truss analogy seems apparently to be a little conservative, however.

According to truss analogy, the positive flexural capacity is obtained from the equation

$$M_{uopos} = A_s \cdot f_{yl} \cdot h_o \quad (25)$$

Thus it is assumed that the internal lever arm $z = h_o$. In this study, flexural capacity is calculated, applying the notation presented in Fig. 3, from the equation

$$M_{uopos} = \int_{A_{cc}} \sigma_c(\epsilon_c) \cdot \frac{\epsilon_c}{\epsilon_{cc}} \cdot x \cdot dA + D_s \cdot (x-d') + Z_s \cdot (d-x) \quad (26)$$

M_{uoneg} is obtained in the same way. The internal stress resultants are obtained within iteration using the equilibrium equation of internal forces of the section.

In pure torsion, the capacity is calculated in accordance with truss analogy from the equation

$$T_{uo} = 2 \cdot A_o \cdot \sqrt{\frac{A_{sl} \cdot f_{yl} \cdot A_{st} \cdot f_{yt}}{u_o \cdot s}} \quad (27)$$

The shear capacity in pure shear is calculated from the equation

$$V_{uo} = \sqrt{\frac{2 \cdot A_{sl} \cdot f_{yl} \cdot h_o \cdot A_{st} \cdot f_{yt}}{s}} \quad (28)$$

Under combined bending, torsion and shear, the failure in a beam section can occur in accordance with three different

failure models:

1. The longitudinal reinforcement of the lower edge, as well as the stirrups, begin to yield first. Thus, the following interactional equation is valid:

$$\frac{M_u}{M_{uo1}} + \left(\frac{T_u}{T_{uo1}}\right)^2 + \left(\frac{V_u}{V_{uo1}}\right)^2 = 1 \quad (29)$$

T_{uo1} is derived from the equation

$$T_{uo1} = 2 \cdot A_o \cdot \sqrt{\frac{2 \cdot A_s \cdot f_{yl} \cdot A_{st} \cdot f_{yt}}{u_o \cdot s}} \quad (30)$$

and V_{uo1} from the equation

$$V_{uo1} = 2 \cdot \sqrt{\frac{A_s \cdot f_{yl} \cdot h_o \cdot A_{st} \cdot f_{yt}}{s}} \quad (31)$$

2. The longitudinal reinforcement of the upper edge, as well as the stirrups, begin to yield first. Then the following interactional equation is valid:

$$\frac{M_u}{M_{uoneg}} + \left(\frac{T_u}{T_{uo2}}\right)^2 + \left(\frac{V_u}{V_{uo2}}\right)^2 = 1 \quad (32)$$

Now we have equations

$$T_{uo2} = 2 \cdot A_o \cdot \sqrt{\frac{2 \cdot A'_s \cdot f_{yl} \cdot A_{st} \cdot f_{yt}}{u_o \cdot s}} \quad (33)$$

$$V_{uo2} = 2 \cdot \sqrt{\frac{A'_s \cdot f_{yl} \cdot h_o \cdot A_{st} \cdot f_{yt}}{s}} \quad (34)$$

3. The longitudinal reinforcement and the stirrups begin to yield first on that side of the section where the shear stresses brought about by shear force and the torsional moment are parallel. Consequently, the following interactional equation is valid:

$$\left(\frac{T_u}{T_{uo3}}\right)^2 + \frac{T_u}{T_{uo3}} \cdot \frac{V_u}{V_{uo3}} \cdot \frac{2}{\sqrt{1 + \frac{b_o}{h_o}}} + \left(\frac{V_u}{V_{uo3}}\right)^2 = 1 \quad (35)$$

T_{u03} is obtained from Eq. (27) and V_{u03} from Eq. (28).

When employing truss analogy, it is assumed that the reinforcement of the beam carries the entire shear force. It is, however, known that also concrete bears part of it. Therefore, in this study, the external shear force V_u in Eqs. (29), (32) and (35) is replaced by that part of it which is carried by the reinforcement: in other words by the difference $V_u - V_c$. V_c is the shear capacity of the concrete section, and it is obtained from the equation

$$V_c = f_{ct} \cdot b_w \cdot z \quad (36)$$

Here

$$z \approx z_{u0} = \frac{|M_{u0}|}{D_c + D_s} = \frac{|M_{u0}|}{Z_s} \quad (37)$$

and f_{ct} is calculated from Eq. (7). If $V_u \geq V_c$, then we notate $V_c = V_u$, at which point the terms in Eqs. (29), (32) and (35), brought about by shear force, are cancelled.

6. RIGIDITY OF A REINFORCED CONCRETE BEAM SECTION

6.1. Flexural rigidity

The flexural rigidity of reinforced concrete beam section is not constant. Because the flexural rigidity is defined in this study by the flexural moment M and the curvature ϕ by the equation

$$\phi = \frac{M}{K_m} \quad , \quad (38)$$

flexural rigidity can be examined by the secant of the ϕ - M diagram. The ϕ - M diagram of the reinforced concrete beam section is a curved line, in which the initiation of cracking in the concrete and tensile steel yielding result in a clear change in its direction. The curved line can be approximated, in accordance with the test results, through the trisegmental moment-curvature relationship as presented schematically in Fig. 4. In pure flexure the diagram $OA_B C$ is used, and in combined loading the diagram $OABC$ is utilized.

Between the points O and A , ϕ - M diagram is curved in such a way that K_m diminishes rectilinearly from the value K_{me} to the value K_{mp0} as M advances from zero to the value M_{r0} . The lines A_B , B_C , AB and BC are straight lines, assuming that the ratio $M^0 : T : V \cdot d$ remains unchanged during loading.

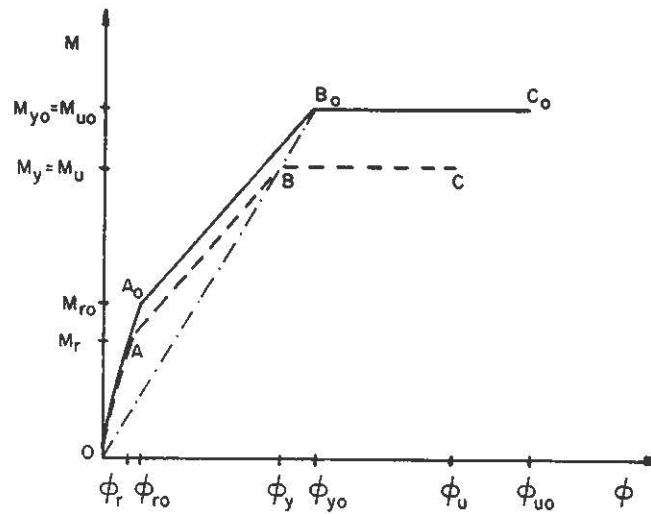


Fig. 4. The reinforced concrete beam curvature-flexural moment model used in this study, presented schematically. Pure flexure ———, combined flexure, torsion and shear - - - - .

6.2. Torsional rigidity

The torsional rigidity is defined as the secant rigidity. Thus we have the equation

$$\theta = \frac{T}{K_t} \tag{39}$$

analogously with the flexural rigidity. Therefore, the torsional rigidity can be examined by the θ -T diagram, when θ is the twist and T the torsional moment. In this investigation, the calculation of the torsional rigidity is founded on the diagram θ -T schematically delineated in Fig. 5. The diagrams θ -T in Fig. 5 are trisegmental in same way as the diagrams ϕ -M in Fig. 4. The line OA_0 in Fig. 5 is curved in such a way that K_t diminishes rectilinearly from the value K_{te} to the value K_{tro} as θ increases from zero to the value θ_{ro} .

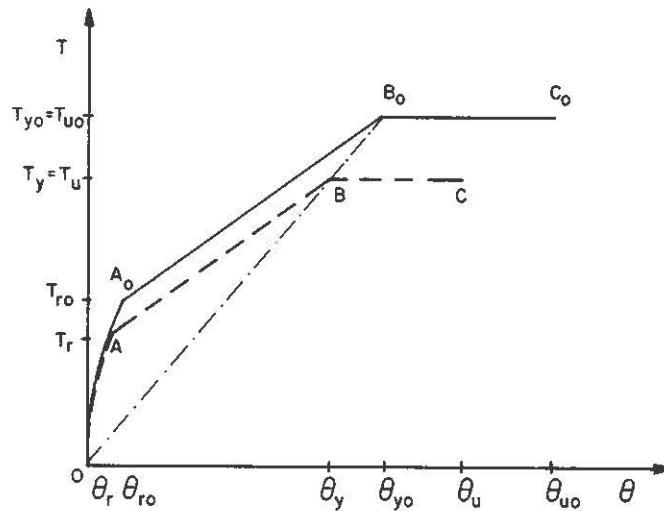


Fig. 5. The reinforced concrete beam twist-torque curve model used in this study, presented schematically. Pure torque ———, combined flexure, torsion and shear - - - - .

As the first cracks in a section appear, flexural or shear cracks, a fold is formed in the point A_0 or A at the same time both in the ϕ - M curve and in the θ - T curve. The fold B_0 or B in both curves is formed at the same time as the yielding of reinforcement begins according to any failure model.

7. METHOD OF ANALYSIS

The analysis of beam grids in this study is founded on the finite element method. The beam parts between the junction points of the beams are viewed as unidimensional beam elements. The degrees of freedom and coordinate systems of an element are presented in Fig. 6.

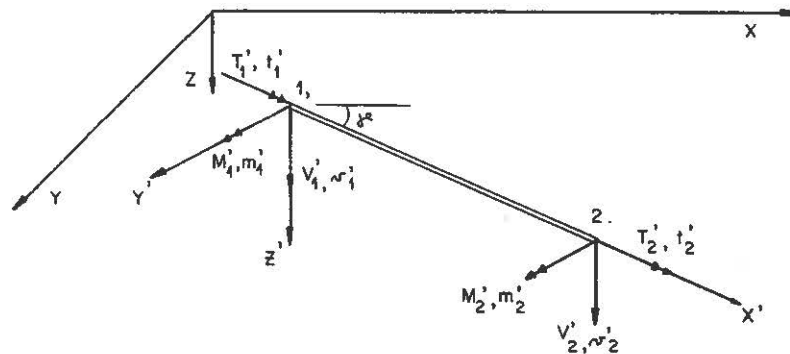


Fig. 6. A beam element, its degrees of freedom and systems of coordinates.

The external load is augmented at the joints in stages. At each loading stage, the displacements and force quantities are calculated through iteration using matrix equation

$$Q = K \cdot \Delta \quad (40)$$

The stiffness matrix of the structure is calculated anew after each iteration as a function of the displacements and force quantities obtained during the preceding iteration cycle. The principle of virtual work, shape function and numerical integration are used in calculation of the stiffness matrix K . The secant rigidity is used for the stiffness of the structure.

The convergence of iteration is audited using the inequation

$$\frac{1}{12 \cdot n} \cdot \sum_1^{6 \cdot n} \cdot \left(\left| \frac{t^{+1} \delta_i^! - t \delta_i^!}{t \delta_i^!} \right| + \left| \frac{t^{+1} F_i^! - t F_i^!}{t F_i^!} \right| \right) < \epsilon \quad (41)$$

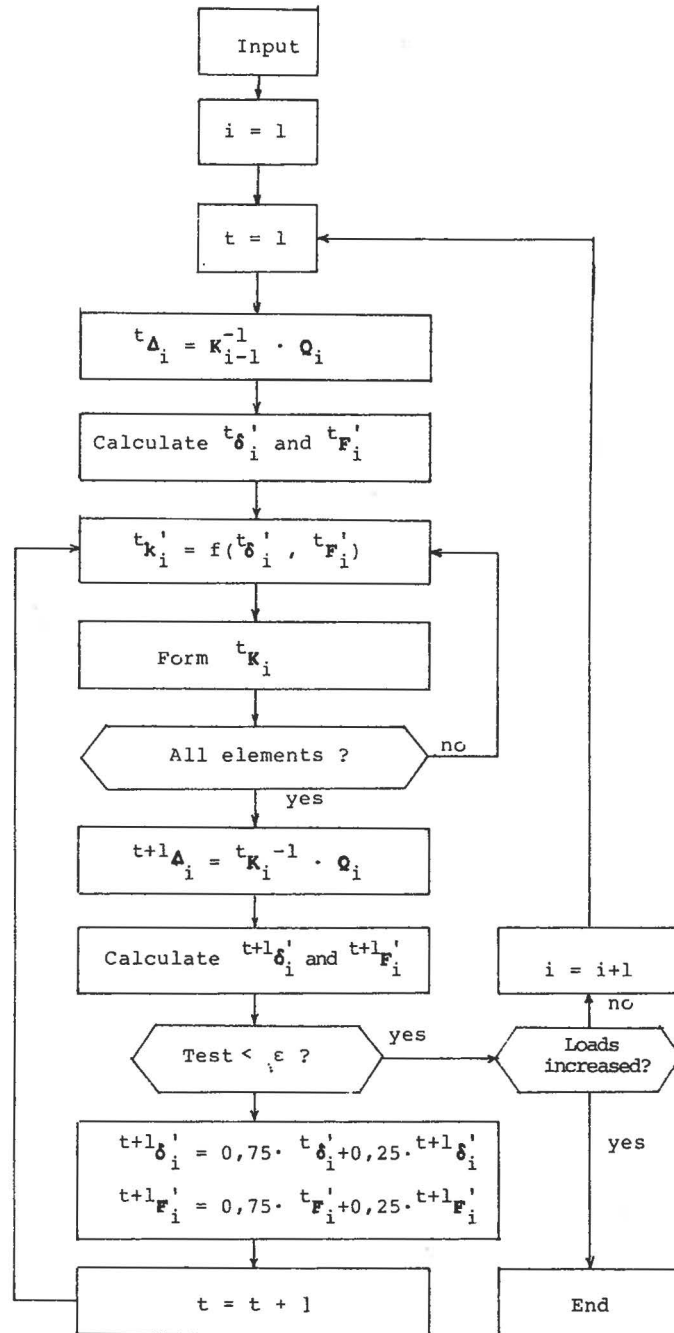
If the Ineq. (41) is invalid the values below are given to the nodal point displacements and forces in reference to the following cycle of iteration

$$t^{+1} \delta_i^! = 0,75 \cdot t \delta_i^! + 0,25 \cdot t^{+1} \delta_i^! \quad (42)$$

$$t^{+1} F_i^! = 0,75 \cdot t F_i^! + 0,25 \cdot t^{+1} F_i^!$$

As the loading increases, the reinforcement begins to yield producing plastic hinges. In the calculation procedure used in this study, the hinges can be formed at the member ends only. They can be flexural, torsional or shear hinges or combinations of these. Finally, due to the plastic hinges, the structure becomes a mechanism and the yield load has been achieved.

The course of calculations in its entirety is demonstrated in the form of a block diagram, as follows:



8. COMPARISON OF EXPERIMENTAL AND THEORETICAL VALUES

In order to test the method of analysis, a test beam grid was made and loaded in connection of this study, the structure and loading system of which are outlined in Ref. /1/. The deflections of the joints of that beam grid are presented in Fig. 7. We can notice that the calculational results concerning deflections and yield load are partly conservative.

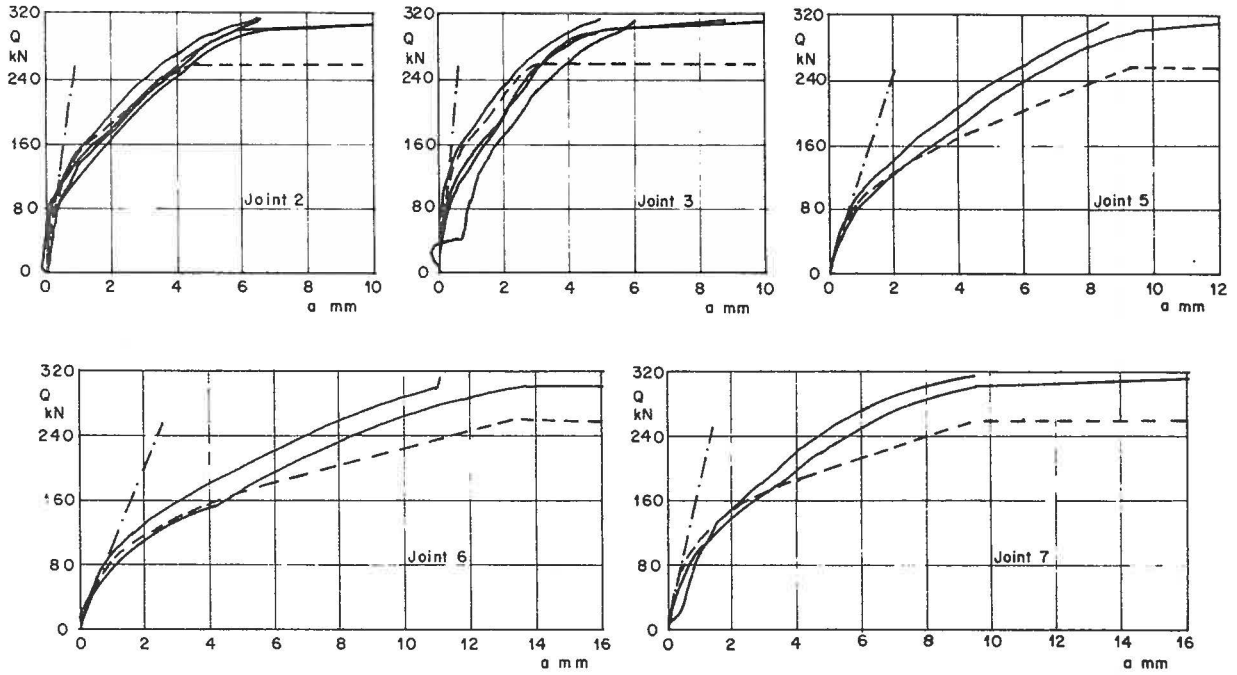


Fig. 7. The deflections experimentally and theoretically obtained for the joints of the test beam grid, as a load function. Test —, nonlinear theory - - -, linear elasticity theory - · - ·.

In Refs. /2/ and /3/, test results of some T-shaped structures consisting of a floor beam and a spandrel beam are reported. The torsional moment, generated in the spandrel beams, was measured in the tests. In Figs. 8 and 9, the calculated torque is compared with the experimental observation. The calculated yield load is noticed to be clearly smaller than the yield load in the tests.

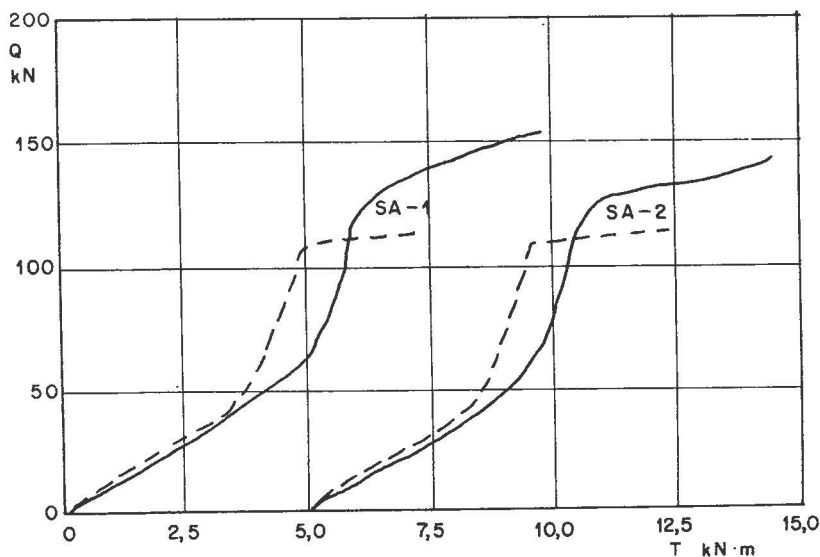


Fig. 8. The experimentally and theoretically obtained torsional moment of a spandrel beam proper to test specimens SA-1 and SA-2 /2/, as a function of load. Test ——— , theory - - - - .

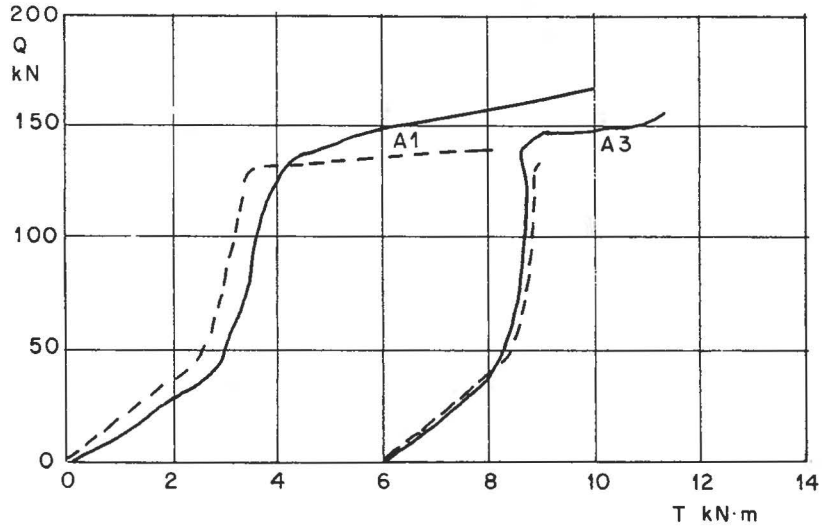


Fig. 9. The experimentally and theoretically obtained torsional moment of the spandrel beam of test specimens A1 and A2 /3/, as a function of load. Test ——— , theory - - - - .

Recharadt & Tiira have loaded some cross-sectionally rectangular-shaped, simply supported beams /4/. Torsion consequently did not appear in the beams. The midpoint deflection of the beams was measured. In Fig. 10, the calculated deflections are compared with the curves obtained experimentally. The correspondence between the theoretical and experimental deflections is very good.

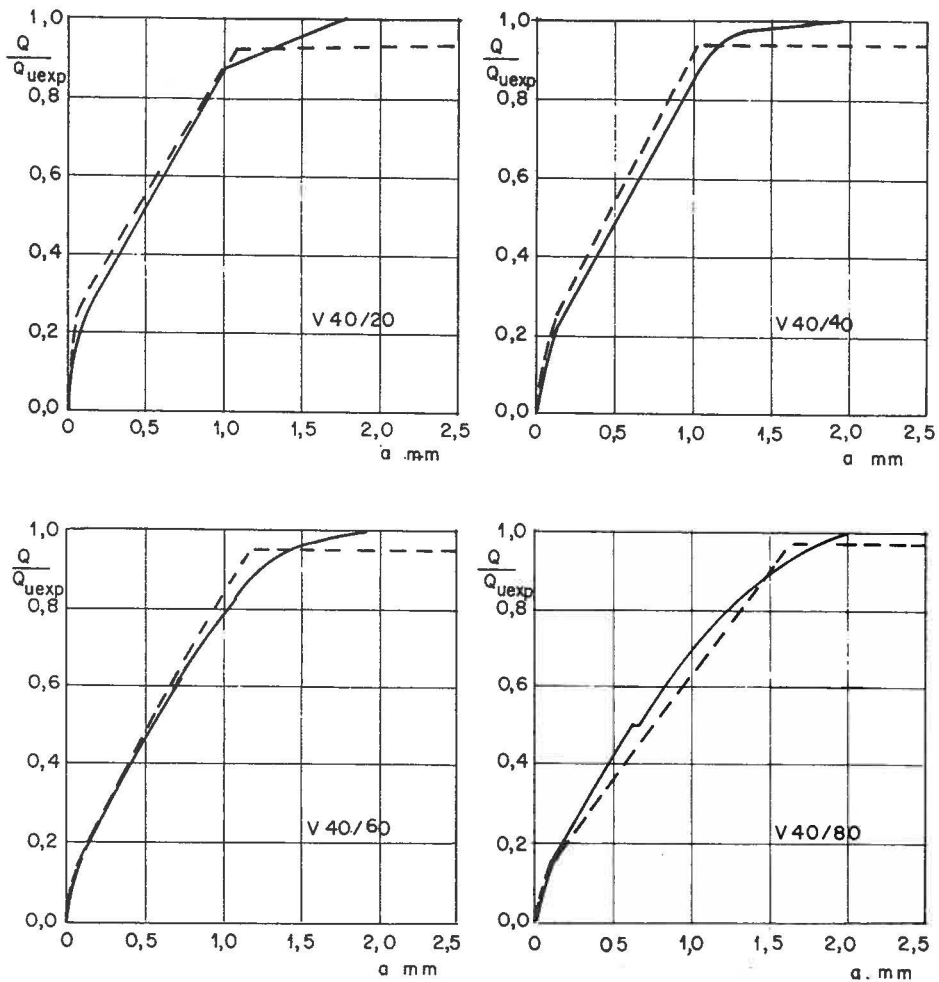


Fig. 10. The experimentally and theoretically obtained mid-point deflections of four test beams, as a function of relative load. Test ———, theory - - - - .

9. CONCLUSIONS

Although, in developing the calculation method, many simplifications and approximations have been made, the calculational findings correlate rather well with the test results. In many cases, however, the calculated results seem to be conservative, mainly due to the multidimensionality of the structure, secondary stresses, biaxial stress state in the slab and ideal-plastic hinges. The disparities obtained among the displacements in calculation and experiment, under the working load, are practically non-existent. The cracking in the concrete appears to start in harmony with the suggested calculation model.

The effect of torque on the behaviour of a beam grid is apparently very minimal. In reality, the torsion would be treated as restrained in character. In considering practical requirements, the compatibility torsion in the beam grids may be ignored, as confirmed frequently in the literature. So the

analysis would be simplified significantly.

The computation time is increased by the fact that the stiffness matrix of the structure is renewed, and the set of equilibrium equations are resolved during each iteration cycle. If the accuracy of iteration is about 0,03, the number of integration points in an element is 5...7 and if the load increment is about 10 % from the yield load, the number of calculation cycles can be kept moderate.

ACKNOWLEDGEMENTS

This research study has been completed at the Institute of Constructions of the Department of Civil Engineering, the University of Oulu, Finland. The writer wishes to express his deepest gratitude to the faculty staff for the assistance he has received. Economic support for this study has been granted by the Foundation for the Advancement of Technology, the Aaltonen Foundation and the Tauno Tönning Foundation. Warm thanks are directed to these sponsors.

REFERENCES

1. Kilpeläinen Mikko, Nonlinear structural analysis of reinforced concrete beam grids. Acta Universitatis Ouluensis. Series C, Technica No 18. Department of Civil Engineering, University of Oulu, Oulu, 1981, 119 p. (dissertation).
2. Mansur M. & Rangan V., Torsion in Spandrel Beams. Journal of Structural Division, ASCE, 104 (1978):7, pp. 1061-1075.
3. Hsu T. & Burton K., Design of Reinforced Concrete Spandrel Beams. Journal of Structural Division, ASCE, 100 (1974):1, pp. 209-229.
4. Rechartdt T. & Tiira S., On the stiffness of the reinforced concrete beam. State Technical Research Centre. Report Series III, Building 82, Helsinki 1965, (Finnish).

SYMBOLS

Scalars

A_{cc}, A_{ct}	area of compressed or tensioned section
A_s, A'_s	area of longitudinal reinforcement of the lower or upper edge of the section
A_{sl}	area of longitudinal reinforcement
A_{st}	area of stirrup
A_o	area of polygon formed by the centres of gravity of the longitudinal stringers located in the corners of the section
K_{me}, K_{te}	flexural or torsional rigidity of section according to theory of linear elasticity
K_{mro}, K_{tro}	flexural or torsional rigidity of section as cracking begins in the concrete in pure flexure or in pure torsion
a	deflection; shear span
b_f	width of flange in torsion
b_o, h_o	horizontal or vertical distance between centres of gravity of the stringers located in the corners of section
f'_c	cylinder strength of concrete
f_{yl}, f_{yt}	yielding strength of longitudinal or transverse reinforcement
i	subscript-indicates load increment
n	number of elements of the beam grid
s	stirrup spacing
t	superscript-indicates iteration cycle during one load increment
u_o	circumference of the area A_o
ϵ	strain; accuracy of iteration
σ_1	principal tensile stress of concrete
τ_t	shear stress brought about by torsion
τ_v	shear stress brought about by shear

Vectors and matrices

F', F	force vector of element in local or global system of coordinates
K	secant stiffness matrix of beam grid
k', k	stiffness matrix of element in local or global

	system of coordinates
Q	load vector of beam grid
Δ	displacement vector of beam grid
δ', δ	displacement vector of element in local or global system of coordinates